EVOLUTION & DEVELOPMENT 17:3, 175–184 (2015)
DOI: 10.1111/ede.12124

# Dual embryonic origin and patterning of the pharyngeal skeleton in the axolotl (*Ambystoma mexicanum*)

**Elizabeth M. Sefton,* Nadine Piekarski, and James Hanken**

Department of Organismic and Evolutionary Biology and Museum of Comparative Zoology, Harvard University, 26 Oxford Street, Cambridge, MA 02138, USA

*Author for correspondence: (esefton@oeb.harvard.edu)

**SUMMARY** The impressive morphological diversification of vertebrates was achieved in part by innovation and modification of the pharyngeal skeleton. Extensive fate mapping in amniote models has revealed a primarily cranial neural crest derivation of the pharyngeal skeleton. Although comparable fate maps of amphibians produced over several decades have failed to document a neural crest derivation of ventromedial elements in these vertebrates, a recent report provides evidence of a mesodermal origin of one of these elements, basibranchial 2, in the axolotl. We used a transgenic labeling protocol and grafts of labeled cells between GFP+ and white embryos to derive a fate map that describes contributions of both cranial neural crest and mesoderm to the axolotl pharyngeal skeleton, and we conducted additional experiments that probe the mechanisms that underlie mesodermal patterning. Our fate map confirms a dual embryonic origin of the pharyngeal skeleton in urodeles, including derivation of basibranchial 2 from mesoderm closely associated with the second heart field. Additionally, heterotopic transplantation experiments reveal lineage restriction of mesodermal cells that contribute to pharyngeal cartilage. The mesoderm-derived component of the pharyngeal skeleton appears to be particularly sensitive to retinoic acid (RA): administration of exogenous RA leads to loss of the second basibranchial, but not the first. Neural crest was undoubtedly critical in the evolution of the vertebrate pharyngeal skeleton, but mesoderm may have played a central role in forming ventromedial elements, in particular. When and how many times during vertebrate phylogeny a mesodermal contribution to the pharyngeal skeleton evolved remain to be resolved.

## INTRODUCTION

The pharyngeal skeleton, an autapomorphy of gnathostomes, has undergone dramatic morphological change across the vertebrate clade (Lauder 1982; Mallatt 1996). In extant fishes and larval amphibians it supports the gills, tongue, and muscles of the pharynx, whereas in adult tetrapods it surrounds the larynx and trachea and contributes to the middle ear. Despite its morphological diversity in gnathostomes, the pharyngeal skeleton is believed to have a highly conserved embryonic origin from cranial neural crest (Creuzet et al., 2005; Knight and Schilling 2006). Indeed, the extensive contribution of neural crest to the pharyngeal skeleton and other cranial tissues (Le Lièvre and Le Douarin 1975; Tan and Morriss-Kay 1986; Langille and Hall 1987; Couly et al., 1993; Platt 1893; Köntges and Lumsden 1996; Mongera et al., 2013) is a primary feature of the "New Head" hypothesis, wherein neural crest functions in the head, similar to mesoderm in the trunk, to generate novel structures associated with a predatory lifestyle (Gans and Northcutt 1983). Moreover, neural crest is a source of interspecific variation in craniofacial morphology, capable of carrying out autonomous developmental programs (Schneider and Helms 2003).

Fate-mapping studies of amphibians, however, have failed to document a neural crest origin of some midline pharyngeal cartilages. In neural crest extirpation experiments in the spotted salamander, *Ambystoma maculatum*, basibranchial 2, a ventromedial element, formed in the absence of neural crest cells (Stone 1926; Fig. S1B). In frogs, neural crest does not contribute to either the basihyal or basibranchial 2, two larval ventromedial cartilages (Stone 1929; Sadaghiani and Thiébaud 1987; Olsson and Hanken 1996). It is unknown whether the absence of a neural crest contribution to midline cartilages represents a derived trait within amphibians or instead represents a character that is more widely distributed among gnathostomes.

Much less is known regarding the long-term lineage of cranial mesoderm in comparison to cranial neural crest, although fate maps of cranial mesoderm have been produced for mouse and chicken (Noden 1988; Couly et al., 1992, 1993; Evans and Noden 2006; McBratney-Owen 2008; Yoshida et al., 2008). Mammals, however, have a highly modified pharyngeal skeleton and lack basibranchials, whereas in the chicken, the basihyal and single basibranchial are derived exclusively from neural crest (Le Lièvre 1978). This begs the question of the embryonic origin of homologous elements in species, such as salamanders, that retain an evolutionarily more ancestral

condition of the pharyngeal skeleton. Such information may provide important insight into the plesiomorphic pattern of development in tetrapods, or even bony fishes. Previous mesodermal fate-mapping studies of the salamander head have described the skeletal and muscular derivatives of individual somites (Piekarski and Olsson 2007), and a recent study reported a mesodermal origin of basibranchial 2 in the axolotl, *Ambystoma mexicanum* (Davidian and Malashichev 2013). Here, we examine mechanisms that mediate pharyngeal skeletal patterning in the axolotl, with particular focus on mesodermal derivatives. To fate map contributions of neural crest and cranial mesoderm to the pharyngeal skeleton, cells are grafted orthotopicaly from GFP+ transgenic donor embryos into white mutant (dd) hosts (Sobkow et al., 2006). In addition, we evaluate the cell potency of cranial mesoderm through heterotopic transplantations. Finally, we evaluate the role of retinoic acid in regulating development of the pharyngeal skeleton during embryogenesis. We discuss our results in a broader context of the evolution of the pharyngeal skeleton.

## MATERIALS AND METHODS

### *Ambystoma mexicanum* embryos

White mutant (dd), GFP+ white mutant and albino (aa) embryos of the Mexican axolotl (*Ambystoma mexicanum*) were obtained from the Ambystoma Genetic Stock Center at the University of Kentucky and from our laboratory breeding colony. Before grafting, embryos were decapsulated manually by using watchmaker forceps. They were staged according to Bordzilovskaya et al. (1989).

### Grafting procedure

In all transplantation experiments, labeled cells were grafted from GFP+ white mutant donor embryos into white mutant (dd) hosts. The donor embryos ubiquitously express GFP under the control of the CAGGS promoter (Sobkow et al., 2006). After dejellying, embryos were transferred into agar-coated dishes (2% agar in 20% Holtfreter solution) containing sterile 100% Holtfreter solution. Operations were carried out with tungsten needles on the left side of the embryo. Explants of individual cranial neural crest streams (stages 15–17) or cranial mesoderm (stages 19–23) from donor embryos were grafted unilaterally into stage-matched hosts whose comparable regions had been extirpated. Donors and hosts were of equivalent size and form. Explants were kept in place with a glass coverslip for the first several minutes to promote healing. Cranial mesoderm has no obvious morphological segments or boundaries; we differentiated graft regions based on the morphology of the overlying neural tube. There is undoubtedly a small amount of overlap between adjacent sections, whose borders are approximate. To avoid contamination with neural crest, cranial mesoderm transplants were carried out before migrating neural crest cells had reached the level of paraxial mesoderm (Piekarski 2009).

Cranial mesoderm cells were grafted heterotopically from GFP+ white mutant donor embryos into stage-matched white mutant (dd) hosts. Transplantations were performed between stages 19 and 22. Host embryos were prepared through a cut into the overlying ectoderm with tungsten needles. Cranial mesoderm cells from regions 1 and 4 of hosts were extirpated (Fig. 2). After removal of overlying donor ectoderm, GFP+ cranial mesoderm cells from regions 5 and 6 were transplanted into regions 1 and 4 of the host (Fig. 2).

### Immunohistochemistry

Chimeric embryos were anaesthetized in tricaine methane–sulfonate (MS-222; Sigma, St. Louis, MO) and fixed in 4% paraformaldehyde in phosphate-buffered saline (PFA/PBS) overnight at 4°C. After washing in PBS, specimens were transferred to 15% sucrose for several hours, followed by 30% sucrose overnight. Specimens were soaked in a 1:1 solution of 30% sucrose and Tissue Tek OCT Embedding Compound (Electron Microscopy Sciences, Hatfield, PA) for several hours. Specimens were embedded in OCT and sectioned at 12–16 μm thickness. Sections were incubated with rabbit polyclonal anti-GFP ab290 (1:2,000; Abcam, Cambridge, MA), followed by AlexaFluor-488 goat anti-rabbit (1:500; Life Technologies, Carlsbad, CA). Sections were also stained with DAPI (0.1–1 μg/ml in PBS) to label cell nuclei. Some sections were stained with the skeletal muscle marker 12/101 monoclonal antibody (1:100; Developmental Studies Hybridoma Bank, Iowa City, IA).

### Retinoic acid treatments

Stock solutions (10 mM) of all-trans retinoic acid (RA; Sigma R2625) were prepared in dimethyl sulfoxide (DMSO). White (dd) axolotls were incubated in the dark with final concentrations of 0.01–0.1 μM RA at indicated stages. Control embryos were incubated in 0.1% DMSO. Whole-mount clearing and staining followed the standard protocol by Klymkowsky and Hanken (1991).

### RNA in situ hybridization

Albino (aa) embryos were used for in situ hybridization. Antisense riboprobes were synthesized from the cloned fragment (DIG RNA labeling kit; Roche Diagnostics, Indianapolis, IN). In situ hybridization was performed as previously described (Henrique et al., 1995), with the addition of an MAB-T wash overnight at 4°C (100 mM maleic acid, 150 mM NaCl, pH 7.5, 0.1% Tween 20). Hybridization was performed at 65°C. The *cyp26b1* forward primer sequence is 5′-CATTCACCGCAACAAGAGAA-3′; the reverse primer is 5′-TTGAGCTCTTGCATGGTCAG-3′. Forward and reverse primers for *islet1* are

5′-CACACCCAACAGCATGGTAG-3′ and 5′-TGCTACAG-GAGACCCAGCTT-3′, respectively.

## RESULTS

### Embryonic derivation of the pharyngeal skeleton

To determine the contributions of both cranial mesoderm and cranial neural crest to the pharyngeal skeleton, we used transgenic axolotls that ubiquitously express GFP under the control of the CAGGS promoter (Sobkow et al., 2006). Fate-mapping individual cranial neural crest streams revealed contributions to all cartilage elements except basibranchial 2 (Fig. 1A–C and M). The mandibular stream forms Meckel's cartilage of the lower jaw (as well as the palatoquadrate cartilage and the anterior portion of the trabecula cranii). The hyoid stream forms elements of the hyoid arch, including the ceratohyal and the anterior portion of basibranchial 1. The branchial streams contribute to the posterior half of basibranchial 1 and to the cerato- and hypobranchials.

We performed orthotopic transplantations of six different regions of cranial mesoderm between GFP+ and white (dd) embryos (Fig. 1L). Cells from regions 5 and 6 contributes to basibranchial 2 ($n = 17$; Fig. 1F and G), corroborating recent fate-mapping results in the axolotl, which show that lateral plate mesoderm gives rise to basibranchial 2 and the heart (Davidian and Malashichev 2013). Cells from regions 5 and 6 overlap with those forming ventral craniofacial muscle in most explants ($n = 11/17$). Regions 5 and 6 likely include lateral splanchnic mesoderm (SpM), a population of cells that, in mouse and chicken, is adjacent to cranial paraxial mesoderm (CPM) and includes precursors of both head musculature and the second heart field (Nathan et al., 2008). The boundary between CPM and SpM is defined by gene expression, including *Nkx2.5*, *Isl1*, and *Fgf10* in SpM, and *Cyp26c1* in CPM (Bothe and Dietrich 2006; Nathan et al., 2008). In the chicken, the boundary between CPM and SpM mesoderm cannot be identified morphologically, as CPM is continuous and indistinguishable from SpM mesoderm (Noden and Francis-West 2006). Similarly, hyoid and branchial arch paraxial mesoderm is continuous with lateral plate mesoderm in the axolotl. In the chicken, SpM contributes to the distal myogenic core of the first branchial arch, which forms the ventral intermandibular muscle (Marcucio and Noden 1999; Noden et al., 1999; Nathan et al., 2008). Formation of the intermandibularis muscle in region 5 and 6 transplants in the axolotl is consistent with labeling of SpM that contributes to the distal cores of the branchial arches. The labeling of basibranchial 2 without labeling of cranial muscle indicates that at least a portion of basibranchial 2 progenitors is distinct from intermandibularis muscle progenitors.

Our results suggest a link between pharyngeal skeleton and second heart field development: in every specimen in which basibranchial 2 is labeled, the heart is also labeled. In most cases ($n = 15/17$), heart labeling is present in the outflow tract, which is formed by the second heart field (Fig. 1H; Lee and Saint-Jeannet 2011). In the mouse, cells from the second heart field form the outflow tract myocardium and contribute to the right ventricle and the venous pole of the heart (Cai et al., 2003), and clonal analysis indicates common lineage relationships between cranial muscles and second heart field derivatives (Lescroart et al., 2010). The second heart field also contributes to the growth of the cardiac tube (Buckingham et al., 2005). In the chicken, neural crest contributes to the septation of the outflow tract (Kuratani and Kirby 1991).

The LIM-homeodomain transcription factor *islet1* is expressed in the second heart field in amphibians as well as amniotes (Cai et al., 2003; Brade et al., 2007). In *Xenopus, nkx2.5* is expressed in a broad domain, including both first and second heart fields, whereas *islet1* is restricted to an anterior and more dorsal region in the heart field beginning at stage 28 (Brade et al., 2007; Gessert and Kühl 2009). To determine the location of the second heart field in the axolotl, we examined expression of *islet1* (Fig. 1I–K). *Islet1* is expressed at stage 17 in the anterior region of the embryo, which includes the heart field. At stage 28, *islet1* is strongly expressed in the ventral hyoid and branchial arches in addition to the more dorsal branchial arches. Based on our fate-mapping data, ventral expression of *islet1* appears to closely overlap the region expected to form both basibranchial 2 and the outflow tract.

Pharyngeal mesoderm cells give rise to both cranial muscle and cardiac progenitors (Tirosh-Finkel et al., 2006). The axolotl mesodermal cardiocraniofacial field thus encompasses a portion of the pharyngeal skeleton in addition to the heart and branchiomeric muscles.

### Heterotopic transplantation of basibranchial 2-forming cells

We performed heterotopic transplantations to evaluate the degree of lineage restriction of cranial mesoderm at early tailbud stages. Cells that contribute to basibranchial 2 (including the posterior portion of region 5 and the anterior part of region 6) were moved anteriorly into regions 1 and 4, which normally do not contribute to the pharyngeal arch skeleton but typically form mandibular arch musculature (Fig. 2A). Heterotopically transplanted cells form anterior musculature, including jaw adductors and the intermandibularis muscle (Fig. 2C and E). Muscles form in most cases ($n = 9/12$), but transplanted cells also form basibranchial 2 as well as the heart in its normal location (Fig. 2B, D–E; $n = 8/12$). No heterotopically transplanted cells contribute to anterior pharyngeal arch structures, such as Meckel's cartilage, which suggests cranial mesoderm cannot replace neural crest as a source of pharyngeal arch skeleton. We cannot rule out a community effect, however, wherein smaller groups of individual basibranchial 2-forming

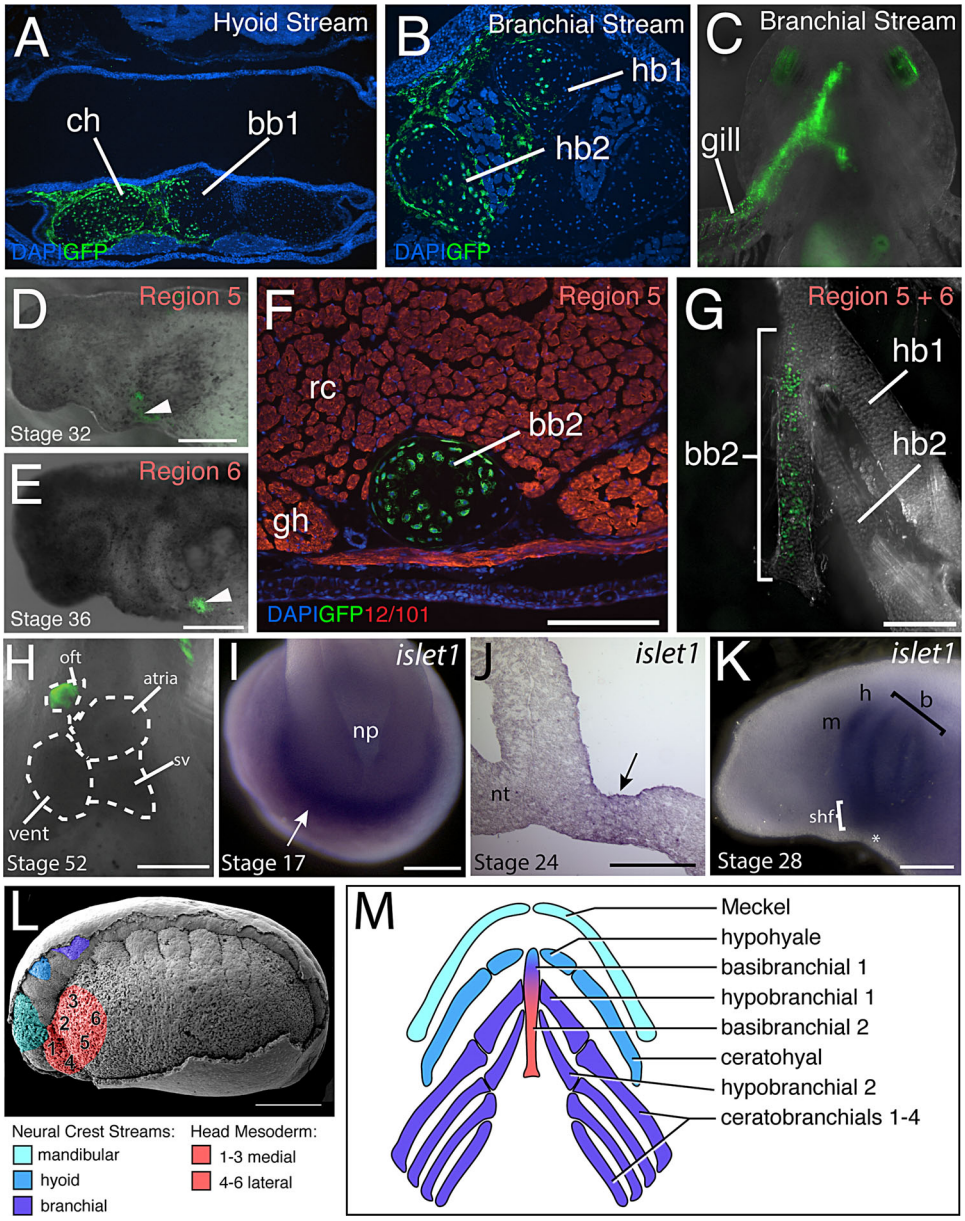


**Fig. 1.** Fate of cranial neural crest and contribution of cranial mesoderm to the pharyngeal skeleton and heart. (A–B) Transverse sections following hyoid and branchial neural crest stream transplantations. (A) Basibranchial 1 (bb1) and the ceratohyal (ch) are labeled following a hyoid stream transplant. (B) Hypobranchials 1 and 2 (hb1, hb2) are labeled following a branchial stream transplant. (C) Ventral view of a branchial stream transplant; anterior is at the top. Labeling is present in the hypobranchial region and the gills. (D) Region 5 mesoderm graft (arrowhead) in a stage-32 embryo after transplantation at stage 19. (E) Region 6 mesoderm graft (arrowhead) in a stage-36 embryo. (F) Transverse section of a region 5-labeled specimen at stage 55. GFP-labeled cells are present in basibranchial 2 (bb2). Muscle (red) is labeled with the 12/101 antibody; nuclei (blue) are stained with DAPI. (G) Dissected pharyngeal skeleton of a stage-46 larva shows labeling of basibranchial 2. Ventral view, anterior is at the top; lateral cartilages have been removed from the right side. (H) Regions 5 and 6 graft in a stage-52 larva. Labeling is visible in the outflow tract (oft) of the heart. Additional heart regions: sv, sinus venosus; vent, ventricle. Ventral view, anterior is at the top. (I–K) *islet1* expression. At stage 17, *islet1* is expressed in the anteriormost region of the embryo, including the cardiac crescent (arrow in I). Anterior view, dorsal is at the top. At stage 24, a parasagittal section shows expression in ventral cranial mesendoderm (arrow in J). Anterior is to the left, dorsal to the top. At stage 28, *islet1* is expressed in the hyoid (h) and branchial (b) arches, with additional strong expression ventral to the arches in the proposed second heart field (shf) region. Asterisk indicates the ventral region of the embryo where *islet1* expression is minimal. Lateral view, anterior is to the left. (L) Scanning electron micrograph of a stage-21 embryo. Overlying ectoderm has been removed from the left side, revealing the mandibular (light blue), hyoid (blue) and branchial (purple) cranial neural crest migratory streams and mesoderm (red). (M) Derivation of the pharyngeal skeleton; ventral view, anterior is at the top. Additional abbreviations: gh, geniohyoideus muscle; m, mandibular arch; nt, neural tube; rc, rectus cervicis muscle. Scale bar: 500 μm.

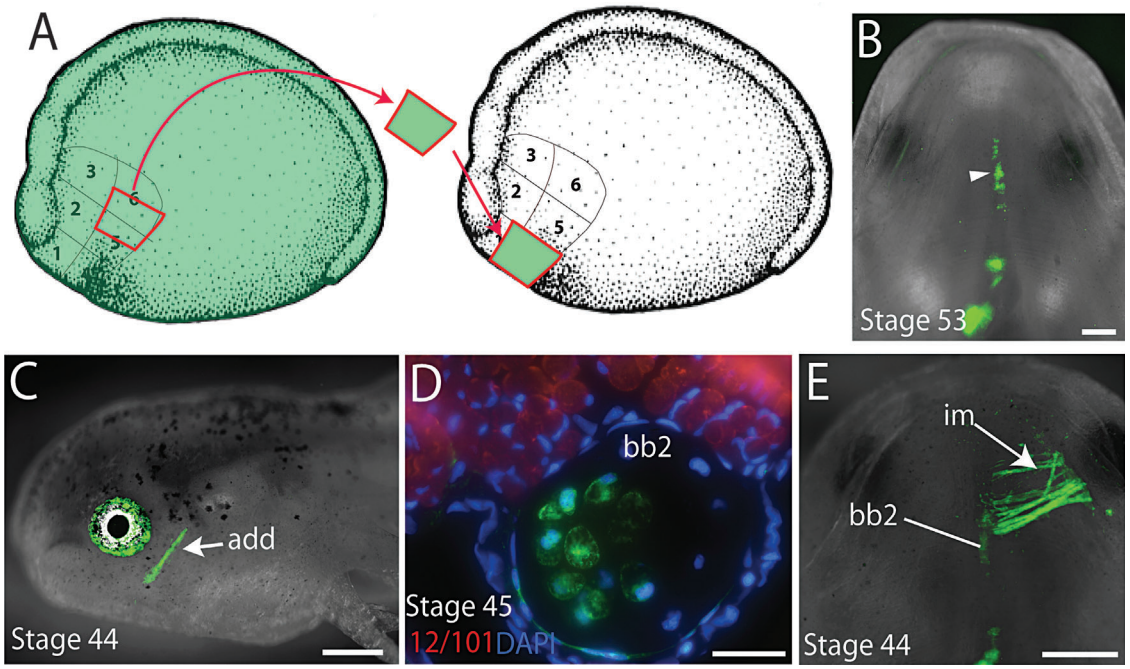


**Fig. 2.** Heterotopic grafting of cranial mesoderm. (A) Drawing of stage-19 embryos illustrating the grafting protocol. Regions 1 and 4 were extirpated from white (dd) hosts and replaced with regions 5 and/or 6 from GFP+ donors. (B) Region 6 graft at stage 53 shows labeling of basibranchial 2 (arrowhead). Ventral view, anterior is at the top. (C) Regions 5 and 6 graft at stage 44 shows labeling of the mandibular levator adductor muscle (add). Lateral view, anterior is to the left. (D) Transverse section of a regions 5 and 6 graft at stage 45 shows labeling of basibranchial 2. Muscle (red) is labeled with the 12/101 antibody; nuclei (blue) are stained with DAPI. (E) Regions 5 and 6 graft at stage 44 shows labeling of basibranchial 2 and the intermandibularis muscle (im). Scale bars: B, C, and E—500 μm; D—100 μm.

cells are more responsive to cues from the host environment, as can occur following transplantation of coherent groups of neural crest cells (Trainor and Krumlauf 2000). Stone (1932) performed heterotopic transplantations of cranial mesoderm (with the surrounding ectoderm and endoderm) into locations in the trunk in the axolotl. These experiments resulted in the formation of ectopic gills, heart and a small rod of cartilage presumed to be basibranchial 2. Development of the ectopic basibranchial 2 was always accompanied by formation of the heart. The lack of positional restriction in the ability of cranial mesoderm to form head muscles by stage 21 in the axolotl agrees with results from comparable studies in mouse: cells transplanted across the anteroposterior axis of CPM generate structures typical of their host location (Trainor et al., 1994).

## Retinoic acid-treated embryos lack basibranchial 2

Proper levels of retinoic acid (RA), a derivative of vitamin A, are required for multiple aspects of craniofacial development (Lohnes et al., 1994; Niederreither and Dolle 2008). To test the role of RA in patterning the axolotl pharyngeal skeleton, we treated embryos with all-trans RA. In zebrafish, excess RA inhibits formation of the posterior basibranchials (Laue et al., 2008). Strikingly, treatment of white (dd) axolotl embryos with 0.05 μM RA results in the absence of basibranchial 2 but not basibranchial 1 ($n = 31/33$; Fig. 3B). Furthermore, all six arches are present with normal anteroposterior patterning (Fig. 3B). Basibranchial 1 remains intact at higher doses ($n = 6/6$; Fig. 3C), whereas even at the lowest dose, 0.01 μM, basibranchial 2, while still present, is less robust than in controls ($n = 9/9$; Fig. S2). This implies that RA restricts basibranchial 2 progenitors. In zebrafish, RA does not have a posteriorizing influence in the location of myocardial progenitors, but instead controls progenitor density (Keegan et al., 2005). *Xenopus* embryos exposed to increased RA before cardiac differentiation have reduced levels of *Nkx2.5* (Jiang et al., 1999). At the low concentrations used in our RA experiments, RA does not appear to have a posteriorizing effect on the pharyngeal skeleton, but instead it has a potent repressive function in the mesoderm-derived component of the axolotl pharyngeal skeleton.

The Cyp26 cytochrome P450 enzymes degrade RA, acting to control RA levels in cells and tissues (reviewed by Blomhoff and Blomhoff 2006). We examined the expression of both *cyp26b1* and *cyp26c1*. Although no significant expression of *cyp26c1* is found in the midline where basibranchial 2 forms (data not shown), *cyp26b1* is expressed in the ventral midline of larvae (Fig. 3D and E). This is consistent with the presence of an

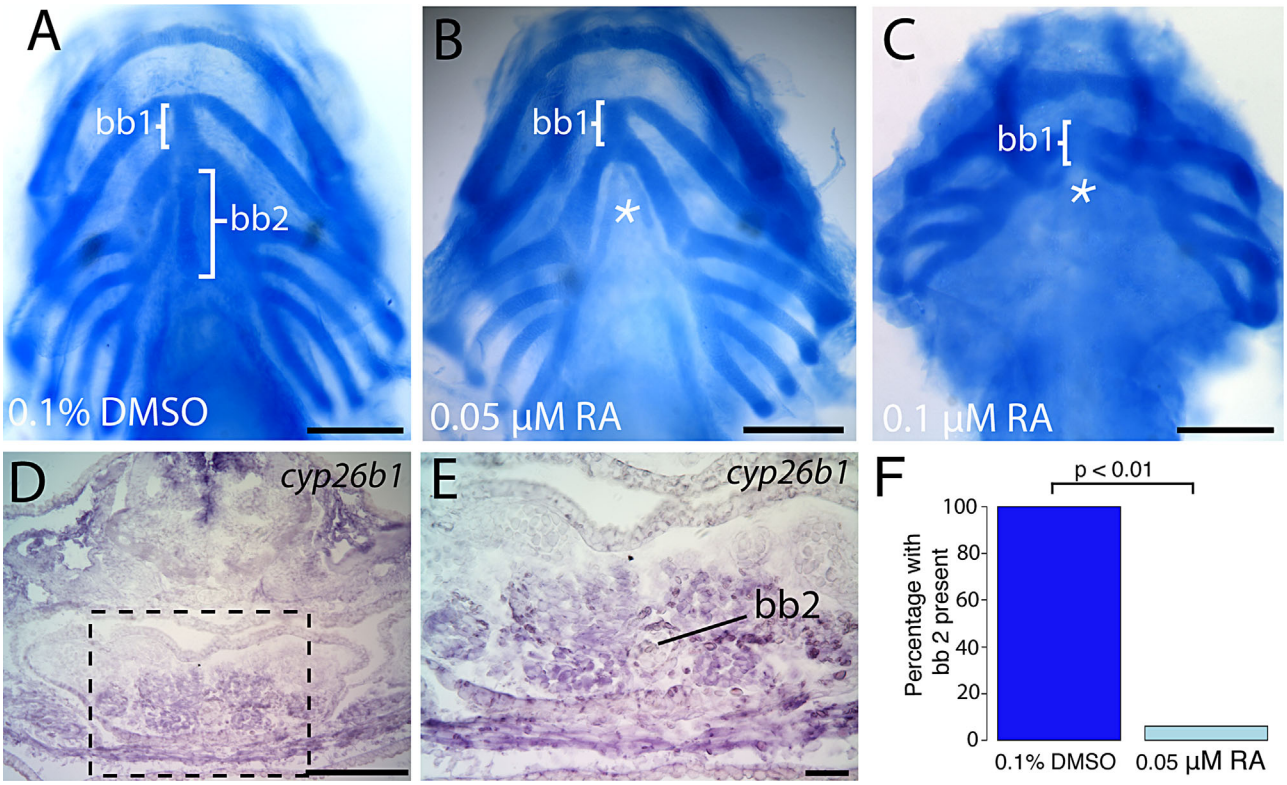


**Fig. 3.** Exogenous retinoic acid (RA) disrupts the mesoderm-derived pharyngeal skeleton. (A–C) Alcian-blue staining of craniofacial cartilages at stage 45 following treatment with 0.1% DMSO (A, control), 0.05 μM RA (B), and 0.1 μM RA (C). Ventral views, anterior is at the top. Brackets depict positions of basibranchials 1 and 2. Asterisks in B and C indicate normal position of missing basibranchial 2. (D and E) Transverse section of a stage-44 *cyp26b1* in situ hybridization. Dashed rectangle in D is enlarged in E. (F) Frequency of basibranchial 2 in control group (0.1% DMSO) and following treatment with 0.05 μM RA. The *P*-value is based on a 2-sample *t*-test.

RA gradient in the head, with concentration increasing from medial to lateral positions (Laue et al., 2008).

## DISCUSSION

### Neural crest-mesoderm boundary in the pharyngeal skeleton

The embryonic derivation of the cranium has significant implications regarding vertebrate origins and relationships (including assessments of skull bone homologies), the flexibility of developmental programs, and the diagnosis and treatment of craniofacial anomalies (Darwin 1859; Kuratani 1997; Kuratani et al., 1997; Schneider 1999; Trainor and Krumlauf 2000; Kimmel et al., 2001; Matsuoka et al., 2005; Cerny et al., 2006). The dual embryonic origin of the skull from both neural crest and mesoderm has been well documented in two widely used amniote models: chicken and mouse. The corresponding pharyngeal skeletons, however, are derived largely from neural crest, and this pattern has generally been extrapolated to all vertebrates. Yet, the pharyngeal skeleton has changed dramatically in the course of vertebrate evolution in relation to feeding, respiration, vocalization and hearing, and amniotes account for only a small portion of that diversity. Fate mapping in multiple lineages is needed to determine the degree to which the neural crest-mesoderm boundary is evolutionarily conservative or labile (Piekarski et al., 2014). Whereas fate mapping and genetic analysis of neural crest has yielded insight into the degree of conservation of embryonic origin and the neural crest-mesoderm boundary in anamniotes (Olsson and Hanken 1996; Horigome et al., 1999; Epperlein et al., 2000; Olsson et al., 2001; Falck et al., 2002; McCauley and Bronner-Fraser 2003, 2006; Ota et al., 2007; Ericsson et al., 2008; Schmidt et al., 2011; Kague et al., 2012; Mongera et al., 2013), fate mapping of cranial mesoderm has received far less attention (Schilling and Kimmel 1994; Kuratani et al., 2004; Davidian and Malashichev 2013). Cranial mesoderm fate maps are particularly important for structures of dual origin, such as the otic capsule and stapes (Noden 1982; Thompson et al., 2012).

The dual embryonic origin of the pharyngeal skeleton in the axolotl provides an additional morphological frontier to study the boundary between neural crest and mesoderm. If the

pharyngeal skeleton is defined to include laryngeal cartilages, then the boundary appears to vary even among amniotes. In the chicken, cricoid, and arytenoid cartilages are derived from lateral mesoderm at the level of the otic placode and first somite, as inferred from quail-chick chimaeras (Noden 1986, 1988) and more recently from retroviral labeling (Evans and Noden 2006). In contrast, genetic fate-mapping in the mouse indicates a neural crest origin of cricoid, arytenoid, and thyroid cartilages (Matsuoka et al., 2005), although aspects of these findings are controversial (Sánchez-Villagra and Maier 2006). Notwithstanding these interspecific differences in its exact location, the neural crest-mesoderm boundary in the pharyngeal skeleton of amniotes is typically placed in the laryngeal cartilages. Our fate mapping in the axolotl, however, shifts the boundary anteriorly to include basibranchial 2, a prominent element in many fishes and amphibians that is absent or significantly transformed in the reduced pharyngeal skeleton of amniotes.

Our heterotopic transplantations suggest that mesoderm that forms basibranchial 2 and the heart is specified earlier in development than mesoderm that forms skeletal muscle. The neural crest-mesoderm boundary remains stable when cartilage-forming mesoderm cells are moved into the mandibular arch; basibranchial 2-forming cells appear unable to form neural-crest derived cartilages following such experimental treatment. And while chondrogenic progenitors maintain their "normal" fate at late-neurula stages, skeletal muscle progenitors demonstrate equivalent potential along the anteroposterior axis. The earlier specification of basibranchial 2 progenitors in the heart field and negative regulation by retinoic acid (RA) offers a potential explanation for the curious absence of neural crest cells from the ventromedial pharyngeal skeleton. Future studies, including clonal analysis, are needed to determine the precise relationship between the second heart field, including the outflow tract, and the formation of basibranchial 2.

## Evolution of basibranchial 2 and the urohyal

Our fate-mapping results confirm the recent report of a mesodermal derivation of basibranchial 2 in the axolotl (Davidian and Malashichev 2013). We further show that cranial mesoderm that forms this cartilage cannot substitute for neural crest in forming other cartilages of the pharyngeal skeleton, and that basibranchial 2 differs from the rest of the pharyngeal skeleton in its response to exogenous RA. These distinctive features of basibranchial 2 are consistent with the hypothesis that this element both develops and evolved independently from the remainder of the pharyngeal skeleton. Jarvik (1963) proposed that basibranchial 2 is not derived from neural crest, but instead forms as a developmental unit with the somite-derived tongue musculature. If this hypothesis is true, then the mesodermal origin of basibranchial 2 and its differential sensitivity to RA may be linked to the somitic signaling environment provided by the surrounding tongue musculature.

According to Jarvik, basibranchial 2 in urodeles is the homolog of the urohyal of piscine sarcopterygians, including the basal taxon *Eusthenopteron*. The urohyal is an unpaired median skeletal element in bony fishes that lies caudal to the basibranchial (Fig. 4). Like basibranchial 2, the urohyal in sarcopterygians forms first as cartilage, which then ossifies endochondrally (Arratia and Schultze 1990). A bony urohyal is also present in teleosts, although it typically forms by intramembranous ossification. In bichirs (*Polypterus* spp.), which are neither teleosts nor sarcopterygians, the urohyal appears to ossify as three distinct ventral tendon bones, although relatively little is known regarding pharyngeal ossification in this evolutionarily conservative sister taxon to all other actinopterygians (Arratia and Schultze 1990). Recent fate-mapping studies demonstrate a neural-crest contribution to the entire pharyngeal skeleton in the zebrafish, including the urohyal (Kague et al., 2012). This result is consistent with the claim that the teleost urohyal, which forms as an ossification of the sternohyoideus tendon, is not homologous to the urohyal of piscine sarcopterygians (Arratia and Schultze 1990). If the zebrafish urohyal is homologous to basibranchial 2 of the axolotl, then developmental system drift (True and Haag 2001) may offer an explanation for the differing germ-layer origin and mode of ossification between these two elements. Given this complex phylogenetic distribution of alternate developmental trajectories and unresolved homologies, we can propose at least three possible scenarios for the evolution of the mesodermal derivation of basibranchial 2 and, possibly, the urohyal (Fig. 4). First, it evolved in basal osteichthyans but later was lost independently in at least some teleosts and amniotes (hypothesis 1). Alternatively, it originated coincident with evolution of endochondral ossification of the urohyal of sarcopterygians and later was lost in at least some amniotes (hypothesis 2). Finally, mesodermal derivation of basibranchial 2 may simply be a synapomorphy unique to urodeles, and possibly other amphibians (hypothesis 3). Parallel, independent evolution of this feature also remains a possibility, if it is present, for example, in piscine sarcopterygians.

Homology of basibranchial 2 and the urohyal, at least across sarcopterygians, is further supported by their strikingly similar morphology. Both basibranchial 2 of the axolotl and the urohyal of the coelacanth are elongate bones that articulate anteriorly with basibranchial 1 and expand caudally to terminate in a bifid tip. Each element also serves as an attachment site for ventral branchial musculature, although the muscle origins and insertions may vary, especially among salamanders (Kleinteich and Haas 2011). For example, the sternohyoideus muscle inserts on the dorsal surface of the urohyal in the coelacanth (Millot and Anthony 1958) and on the dorsal side of basibranchial 2 in the axolotl (Piekarski and Olsson 2007). In the absence of lineage-tracing data from piscine sarcopterygians, hypotheses 2 and 3 are equally parsimonious. Nevertheless, we favor hypothesis 2, primarily because it associates two developmental innovations

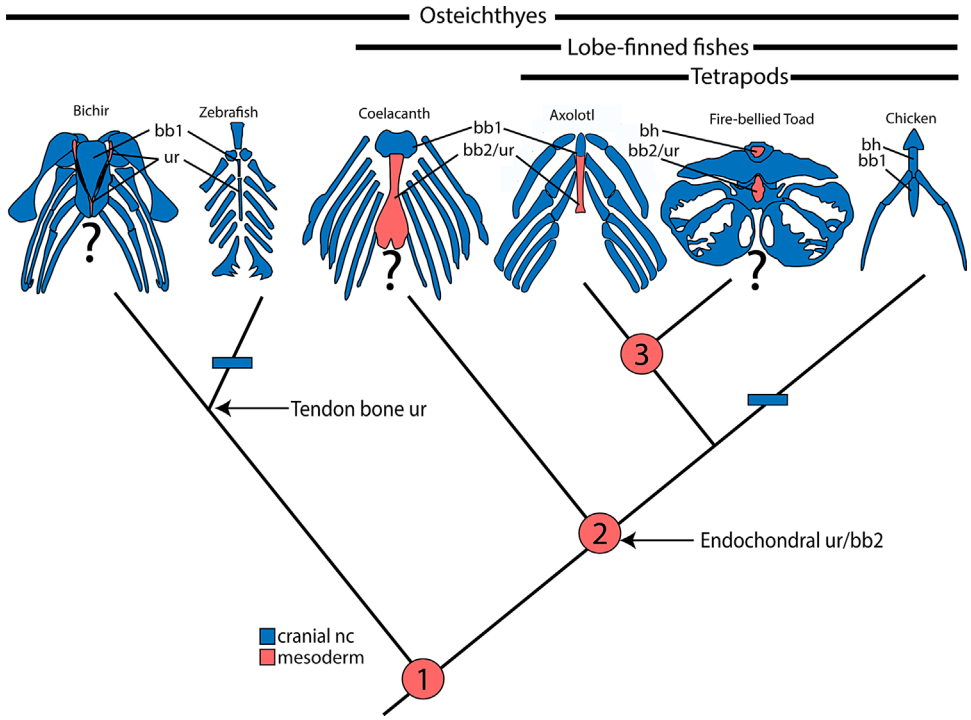


**Fig. 4.** Evolution of pharyngeal skeleton origins. Simplified osteichthyan phylogeny depicting cranial neural crest and cranial mesoderm contributions to the hyoid and branchial arches. The mesodermal contributions to coelacanth (modified from Forey, 1998), toad and bichir (modified from Arratia and Schultze, 1990) are hypothesized (question marks). Red circles represent gain of mesodermal contribution to the pharyngeal skeleton in three alternate hypotheses. Blue bars indicate loss of mesodermal contribution according to hypothesis 1 or 2. The urohyal in teleosts and bichirs, which forms by intramembranous ossification within tendon ("Tendon bone ur"), may not be homologous to the urohyal in sarcopterygians, which ossifies endochondrally within cartilage ("Endochondral ur/bb2"). In hypothesis 1, derivation of bb2/ur from cranial mesoderm is an osteichthyan synapomorphy, which later was lost independently in teleosts (e.g., zebrafish) and amniotes (chicken). In hypothesis 2, mesodermal contribution to the pharyngeal skeleton is a sarcopterygian synapomorphy, which later was lost in amniotes. In hypothesis 3, mesodermal contribution to the pharyngeal skeleton is an amphibian synapomorphy.

at the origin of sarcopterygians: mesodermal origin of median elements of the pharyngeal skeleton, and endochondral ossification of the urohyal/basibranchial 2. If this hypothesis is correct, then these features represent the ancestral condition for lobe-finned fishes. A specific prediction that follows is the mesodermal derivation of the urohyal in piscine sarcopterygians. If the urohyal of teleosts is not homologous to the urohyal of sarcopterygians (Arratia and Schultz 1990), then such a distinctive mode of development of the urohyal of sarcopterygians and the basibranchial 2 of urodeles would not require an evolutionary change in the embryonic derivation of homologous elements. Rather, the urohyal preformed in cartilage would represent a neomorphic element unique to sarcopterygians that evolved by incorporating cranial mesoderm closely associated with the heart field.

Neural crest has played a critical role in vertebrate craniofacial development and evolution (Northcutt 2005; Abitua et al., 2012). According to the "New Head" hypothesis, the origin of the head during the transition of vertebrates to active predation from a more passive protochordate ancestor involved morphological innovations derived from the neural crest and epidermal placodes, as well as muscularization of lateral plate mesoderm (Gans and Northcutt 1983). Neural crest derivation of the pharyngeal skeleton in general has been known for well over a century (Platt 1893). Basibranchial 2 of the axolotl, however, is a surprising example of a functional component of the pharyngeal feeding apparatus that originates instead from cranial mesoderm. In aquatic feeding salamanders, basibranchial 2 is the attachment site of muscles that pull the center of the hyobranchial apparatus forward and open the mouth (Deban and Wake 2000). It is an interesting exception to the more typical association of neural crest with skeletal structures involved in feeding. Tracing its origin and phylogenetic diversity sheds light on whether basibranchial 2 was always linked to the neural crest-derived pharyngeal skeleton, or, if it was not, on how this element came to be integrated with the pharyngeal skeleton following its initial evolution.

## Acknowledgments

We thank Zahra Mohaddeskhorassani for assistance with sectioning, Zachary Lewis for discussion of heart morphology, and Cassandra Extavour for discussion and comments on the manuscript. We are

grateful to Anne Everly, Joanna Larson, and Melissa Aja for their expert animal husbandry. This research was supported by the U.S. National Science Foundation (EF-033484–AmphibiaTree) to J.H.

## Conflict of interest

The authors declare no competing financial interests.

## Author contributions

E.M.S., N.P., and J.H. conceived and designed the experiments. E.M.S. and N.P. performed experiments and analyzed data. E.M.S., J.H., and N.P. wrote the manuscript.

## References

Abitua, P. B., Wagner, E., Navarrete, I. A. and Levine, M. 2012. Identification of a rudimentary neural crest in a non-vertebrate chordate. *Nature* 492: 104–107.

Arratia, G. and Schultze, H. P. 1990. The urohyal: development and homology within osteichthyans. *J. Morphol.* 203: 247–282.

Blomhoff, R. and Blomhoff, H. K. 2006. Overview of retinoid metabolism and function. *J. Neurobiol.* 66: 606–630.

Bordzilovskaya, N. P., Dettlaff, T. A., Duhon, S. T. and Malacinski, G. M. 1989. Developmental-stage series of axolotl embryos. In: J. B. Armstrong and G. M. Malacinski (eds.). *Developmental biology of the Axolotl*. Oxford, Oxford University Press, pp. 201–219.

Bothe, I. and Dietrich, S. 2006. The molecular setup of the avian head mesoderm and its implication for craniofacial myogenesis. *Dev. Dynam.* 235: 2845–2860.

Brade, T., Gessert, S., Kühl, M. and Pandur, P. 2007. The amphibian second heart field: *Xenopus* islet-1 is required for cardiovascular development. *Dev. Biol.* 311: 297–310.

Buckingham, M., Meilhac, S. and Zaffran, S. 2005. Building the mammalian heart from two sources of myocardial cells. *Nat. Rev. Genet.* 6: 826–835.

Cai, C. L., et al. 2003. Isl1 identifies a cardiac progenitor population that proliferates prior to differentiation and contributes a majority of cells to the heart. *Dev. Cell.* 5: 877–889.

Cerny, R., Horáček, I. and Olsson, L. 2006. The trabecula cranii: development and homology of an enigmatic vertebrate head structure. *Anim. Biol.* 56: 503–518.

Couly, G. F., Coltey, P. M. and Le Douarin, N. M. 1992. The developmental fate of the cephalic mesoderm in quail-chick chimeras. *Development* 114: 1–15.

Couly, G. F., Coltey, P. M. and Le Douarin, N. M. 1993. The triple origin of skull in higher vertebrates: a study in quail-chick chimeras. *Development* 117: 409–429.

Creuzet, S., Couly, G. and Le Douarin, N. M. 2005. Patterning the neural crest derivatives during development of the vertebrate head: insights from avian studies. *J. Anat.* 207: 447–459.

Darwin, C. 1859. *On the origin of species*. Murray, London.

Davidian, A. and Malashichev, Y. 2013. Dual embryonic origin of the hyobranchial apparatus in the Mexican axolotl (*Ambystoma mexicanum*). *Int. J. Dev. Biol.* 57: 821–828.

Deban, S. M. and Wake, D. B. 2000. Aquatic feeding in salamanders. *Feeding: form, function and evolution in tetrapod vertebrates*. In: K. Schwenk (ed.). San Diego: Academic Press, pp. 65–94.

Epperlein, H.-H., Meulemans, D., Bronner-Fraser, M., Steinbeisser, H. and Selleck, M. A. J. 2000. Analysis of cranial neural crest migratory pathways in axolotl using cell markers and transplantation. *Development* 127: 2751–2761.

Ericsson, R., Joss, J. and Olsson, L. 2008. The fate of cranial neural crest cells in the Australian lungfish, *Neoceratodus forsteri*. *J. Exp. Zool. B* 310: 345–354.

Evans, D. J. R. and Noden, D. M. 2006. Spatial relations between avian craniofacial neural crest and paraxial mesoderm cells. *Dev. Dynam.* 235: 1310–1325.

Falck, P., Hanken, J. and Olsson, L. 2002. Cranial neural crest emergence and migration in the Mexican axolotl (*Ambystoma mexicanum*). *Zoology* 105: 195–202.

Forey, P. L. 1998. *History of the coelacanth fishes*. Chapman and Hall, London.

Gans, C. and Northcutt, R. G. 1983. Neural crest and the origin of vertebrates: a new head. *Science* 220: 268–273.

Gessert, S. and Kühl, M. 2009. Comparative gene expression analysis and fate mapping studies suggest an early segregation of cardiogenic lineages in *Xenopus laevis*. *Dev. Biol.* 334: 395–408.

Horigome, N., Myojin, M., Ueki, T., Hirano, S., Aizawa, S. and Kuratani, S. 1999. Development of cephalic neural crest cells in embryos of *Lampetra japonica*, with special reference to the evolution of the jaw. *Dev. Biol.* 207: 287–308.

Jarvik, E. 1963. The composition of the intermandibular division of the head in fish and tetrapods and the diphyletic origin of the tetrapod tongue. *Kung. Svensk. Vetens. Handl.* 4: 1–74.

Jiang, Y., Drysdale, T. A. and Evans, T. 1999. A role for GATA-4/5/6 in the regulation of Nkx2.5 expression with implications for patterning of the precardiac field. *Dev. Biol.* 216: 57–71.

Kague, E., Gallagher, M., Burke, S., Parsons, M., Franz-Odendaal, T. and Fisher, S. 2012. Skeletogenic fate of zebrafish cranial and trunk neural crest. *PLoS ONE* 7: e47394.

Keegan, B. R., Feldman, J. L., Begemann, G., Ingham, P. W. and Yelon, D. 2005. Retinoic acid signaling restricts the cardiac progenitor pool. *Science* 307: 247–249.

Kimmel, C. B., Miller, C. T. and Keynes, R. J. 2001. Neural crest and the evolution of the jaw. *J. Anat.* 199: 105–119.

Kleinteich, T. and Haas, H. 2011. The hyal and ventral branchial muscles in caecilian and salamander larvae: homologies and evolution. *J. Morphol.* 272: 598–613.

Klymkowsky, M. W. and Hanken, J. 1991. Whole-mount staining of *Xenopus* and other vertebrates. *Methods Cell Biol.* 36: 419–441.

Knight, R. D. and Schilling, T. F. 2006. Cranial neural crest and development of the head skeleton. *Adv. Exp. Med. Biol.* 589: 120–133.

Köntges, G. and Lumsden, A. 1996. Rhombencephalic neural crest segmentation is preserved throughout craniofacial ontogeny. *Development* 122: 3229–3242.

Kuratani, S. 1997. Spatial distribution of postotic crest cells defines the head/trunk interface of the vertebrate body: embryological interpretation of peripheral nerve morphology and evolution of the vertebrate head. *Anat. Embryol.* 195: 1–13.

Kuratani, S. C. and Kirby, M. L. 1991. Initial migration and distribution of the cardiac neural crest in the avian embryo: an introduction to the concept of the circumpharyngeal crest. *Am. J. Anat.* 191: 215–227.

Kuratani, S., Matsuo, I. and Aizawa, S. 1997. Developmental patterning and evolution of the mammalian viscerocranium. *Dev. Dynam.* 209: 139–155.

Kuratani, S., Murakami, Y., Nobusada, Y., Kusakabe, R. and Hirano, S. 2004. Developmental fate of the mandibular mesoderm in the lamprey, *Lethenteron japonicum*: comparative morphology and development of the gnathostome jaw with special reference to the nature of the trabecula cranii. *J. Exp. Zool. B* 302: 458–468.

Langille, R. and Hall, B. 1987. Development of the head skeleton of the Japanese medaka, *Oryzias latipes* (Teleostei). *J. Morphol.* 193: 135–158.

Lauder, G. V. 1982. Patterns of evolution in the feeding mechanism of actinopterygian fishes. *Integr. Comp. Biol*. 22: 275–285.

Laue, K., Jänicke, M., Plaster, N., Sonntag, C. and Hammerschmidt, M. 2008. Restriction of retinoic acid activity by Cyp26b1 is required for proper timing and patterning of osteogenesis during zebrafish development. *Development* 135: 3775–3787.

Le Lièvre, C. S. 1978. Participation of neural crest-derived cells in the genesis of the skull in birds. *J. Embryol. Exp. Morphol.* 47: 17–37.

Le Lièvre, C. S. and Le Douarin, N. M. 1975. Mesenchymal derivatives of the neural crest: analysis of chimaeric quail and chick embryos. *J. Embryol. Exp. Morphol.* 34: 125–154.

Lee, Y.-H. and Saint-Jeannet, J.-P. 2011. Cardiac neural crest is dispensable for outflow tract septation in *Xenopus*. *Development* 138: 2025–2034.

Lescroart, F., Kelly, R. G., Le Garrec, J.-F., Nicolas, J.-F., Meilhac, S. M. and Buckingham, M. 2010. Clonal analysis reveals common lineage relationships between head muscles and second heart field derivatives in the mouse embryo. *Development* 137: 3269–3279.

Lohnes, D., et al. 1994. Function of the retinoic acid receptors (RARs) during development. (I) Craniofacial and skeletal abnormalities in RAR double mutants. *Development* 120: 2723–2748.

Mallatt, J. 1996. Ventilation and the origin of jawed vertebrates: a new mouth. *Zool. J. Linn. Soc.* 117: 329–404.

Marcucio, R. S. and Noden, D. M. 1999. Myotube heterogeneity in developing chick craniofacial skeletal muscles. *Dev. Dynam.* 214: 178–194.

Matsuoka, T., et al. 2005. Neural crest origins of the neck and shoulder. *Nature* 436: 347–355.

McBratney-Owen, B., Iseki, S., Bamforth, S. D., Olsen, B. R. and Morriss-Kay, G. M. 2008. Development and tissue origins of the mammalian cranial base. *Dev. Biol.* 322: 121–132.

McCauley, D. W. and Bronner-Fraser, M. 2003. Neural crest contributions to the lamprey head. *Development* 130: 2317–2327.

McCauley, D. W. and Bronner-Fraser, M. 2006. Importance of SoxE in neural crest development and the evolution of the pharynx. *Nature* 441: 750–752.

Millot, J., and Anthony, J. 1958. *Anatomie de Latimeria chalumnae. Vol I. Squellete, muscles et formation de soutien*. Centre Nationale de la Recherche Scientifique, Paris.

Mongera, A., Singh, A. P., Levesque, M. P., Chen, Y.-Y., Konstantinidis, P. and Nüsslein-Volhard, C. 2013. Genetic lineage labeling in zebrafish uncovers novel neural crest contributions to the head, including gill pillar cells. *Development* 140: 916–925.

Nathan, E., et al. 2008. The contribution of Islet1-expressing splanchnic mesoderm cells to distinct branchiomeric muscles reveals significant heterogeneity in head muscle development. *Development* 135: 647–657.

Niederreither, K. and Dollé, P. 2008. Retinoic acid in development: towards an integrated view. *Nat. Rev. Genet.* 9: 541–553.

Noden, D. M. 1982. Patterns and organization of craniofacial skeletogenic and myogenic mesenchyme: a perspective. *Factors and mechanisms influencing bone growth*. In: A. D. Dixon and B. Sarnat (eds.). Alan R. Liss, Inc, New York. pp. 167–203.

Noden, D. M. 1986. Origins and patterning of craniofacial mesenchymal tissues. *J Craniofac. Genet. Dev. Biol.* 2: 15–31.

Noden, D. M. 1988. Interactions and fates of avian craniofacial mesenchyme. *Development* 103: 121–140.

Noden, D. M. and Francis-West, P. 2006. The differentiation and morphogenesis of craniofacial muscles. *Dev. Dynam.* 235: 1194–1218.

Noden, D. M., Marcucio, R., Borycki, A. G. and Emerson, C. P. 1999. Differentiation of avian craniofacial muscles: I. Patterns of early regulatory gene expression and myosin heavy chain synthesis. *Dev. Dynam.* 216: 96–112.

Northcutt, R. G. 2005. The new head hypothesis revisited. *J. Exp. Zool.* B304: 274–297.

Olsson, L., Falck, P., Lopez, K., Cobb, J. and Hanken, J. 2001. Cranial neural crest cells contribute to connective tissue in cranial muscles in the anuran amphibian, *Bombina orientalis*. *Dev. Biol.* 237: 354–367.

Olsson, L. and Hanken, J. 1996. Cranial neural-crest migration and chondrogenic fate in the Oriental fire-bellied toad *Bombina orientalis*: defining the ancestral pattern of head development in anuran amphibians. *J. Morphol.* 229: 105–120.

Ota, K. G., Kuraku, S. and Kuratani, S. 2007. Hagfish embryology with reference to the evolution of the neural crest. *Nature* 446: 672–675.

Piekarski, N. 2009. *A long-term fate map of the anterior somites in the Mexican axolotl (Ambystoma mexicanum)*. Unpubl. PhD Dissertation. Friedrich Schiller University of Jena, Germany.

Piekarski, N., Gross, J. B. and Hanken, J. 2014. Evolutionary innovation and conservation in the embryonic derivation of the vertebrate skull. *Nat. Comm.* 5: 5661.

Piekarski, N. and Olsson, L. 2007. Muscular derivatives of the cranialmost somites revealed by long-term fate mapping in the Mexican axolotl (*Ambystoma mexicanum*). *Evol. Dev.* 9: 566–578.

Platt, J. B. 1893. Ectodermic origin of the cartilages of the head. *Anat. Anz.* 8: 506–509.

Sadaghiani, B. and Thiébaud, C. H. 1987. Neural crest development in the *Xenopus laevis* embryo, studied by interspecific transplantation and scanning electron microscopy. *Dev. Biol.* 124: 91–110.

Sánchez-Villagra, M. R. and Maier, W. 2006. Homologies of the mammalian shoulder girdle: a response to Matsuoka et al. *Evol. Dev.* 8: 113–115.

Schilling, T. F. and Kimmel, C. B. 1994. Segment and cell type lineage restrictions during pharyngeal arch development in the zebrafish embryo. *Development* 120: 483–494.

Schmidt, J., Schuff, M. and Olsson, L. 2011. A role for FoxN3 in the development of cranial cartilages and muscles in *Xenopus laevis* (Amphibia: Anura: Pipidae) with special emphasis on the novel rostral cartilages. *J. Anat.* 218: 226–242.

Schneider, R. A. 1999. Neural crest can form cartilages normally derived from mesoderm during development of the avian head skeleton. *Dev. Biol.* 208: 441–455.

Schneider, R. A. and Helms, J. A. 2003. The cellular and molecular origins of beak morphology. *Nature* 299: 565–568.

Sobkow, L., Epperlein, H.-H., Herklotz, S., Straube, W. L. and Tanaka, E. M. 2006. A germline GFP transgenic axolotl and its use to track cell fate: dual origin of the fin mesenchyme during development and the fate of blood cells during regeneration. *Dev. Biol.* 290: 386–397.

Stone, L. S. 1926. Further experiments on the extirpation and transplantation of mesectoderm in *Amblystoma punctatum*. *J. Exp. Zool.* 44: 95–131.

Stone, L. S. 1929. Experiments showing the role of migrating neural crest (mesectoderm) in the formation of head skeleton and loose connective tissue in *Rana palustris*. *Roux Arch. Dev. Biol.* 118: 40–77.

Stone, L. S. 1932. Transplantation of hyobranchial mesentoderm, including the right lateral anlage of the second basibranchium, in *Amblystoma punctatum*. *J. Exp. Zool.* 62: 109–123.

Tan, S. S. and Morriss-Kay, G. M. 1986. Analysis of cranial neural crest cell migration and early fates in postimplantation rat chimaeras. *J. Embryol. Exp. Morphol.* 98: 21–58.

Thompson, H., Ohazama, A., Sharpe, P. T. and Tucker, A. S. 2012. The origin of the stapes and relationship to the otic capsule and oval window. *Dev. Dynam.* 241: 1396–1404.

Tirosh-Finkel, L., Elhanany, H., Rinon, A. and Tzahor, E. 2006. Mesoderm progenitor cells of common origin contribute to the head musculature and the cardiac outflow tract. *Development* 133: 1943–1953.

Trainor, P. and Krumlauf, R. 2000. Plasticity in mouse neural crest cells reveals a new patterning role for cranial mesoderm. *Nat. Cell. Biol.* 2: 96–102.

Trainor, P. A., Tan, S. S. and Tam, P. P. 1994. Cranial paraxial mesoderm: regionalisation of cell fate and impact on craniofacial development in mouse embryos. *Development* 120: 2397–2408.

True, J. R. and Haag, E. S. 2001. Developmental system drift and flexibility in evolutionary trajectories. *Evol. Dev.* 3: 109–119.

Yoshida, T., Vivatbutsiri, P., Morriss-Kay, G., Saga, Y. and Iseki, S. 2008. Cell lineage in mammalian craniofacial mesenchyme. *Mech. Dev.* 125: 797–808.

## SUPPORTING INFORMATION

Additional supporting information may be found in the online version of this article at the publisher's web-site.

**Fig S1**: Fate map and morphology of the salamander pharyngeal skeleton.

**Fig S2**: Effect of retinoic acid (RA) on pharyngeal skeleton morphology.